



ICRC
The Astroparticle Physics Conference
34th International Cosmic Ray Conference
July 30 - August 6, 2015
The Hague, The Netherlands

Measurements of X_{\max} above 10^{17} eV with the fluorescence detector of the Pierre Auger Observatory

CR-EX 1176 – PoS 420

31st July, 2015

Alessio Porcelli^a on behalf of Pierre Auger Collaboration^b

^aKarlsruhe Institute of Technology, Karlsruhe, Germany,

currently in Department of Nuclear Physics, University of Geneva, Geneva, Switzerland

^bObservatorio Pierre Auger, Av. San Martín Norte 304, 5613 Malargüe, Argentina

(full author list: http://www.auger.org/archive/authors_2015_06.html)

Dataset

2 independent datasets:

Standard dataset (18382 events)

- ▶ Known by the scientific community (Phys.Rev. D90 12 (2014) 122005 [[1409.4809v3](#)])
- ▶ Measurement only down to $10^{17.8}$ eV
- ▶ Period between 01.12.2004 and 31.12.2012
- ▶ 24 fluorescence telescopes with 2° to 30° FoV in elevation at 4 sites:
Los Leones (LL), Loma Amarilla (LA), Los Morados (LM), Coihueco (CO)
- ▶ All non-HeCo events (see below)

HeCo dataset (5490 events)

- ▶ Energy span: $10^{17} \leq E \leq 10^{18.3}$ eV
- ▶ Period between 01.06.2010 and 15.08.2012
- ▶ 6 standard fluorescence telescopes at CO sites
- ▶ 3 High Elevation Auger Telescopes (**HEAT**)

HEAT (High Elevation Auger Telescopes)



3 fluorescence telescopes with a sampling 2 times faster than standard.

Operation in downward (left) and upward (right) modes:

2° to 30° FoV in elevation



30° to 60° FoV in elevation



Data Set

Analysis method

Systematic Uncertainties

Results

Conclusions

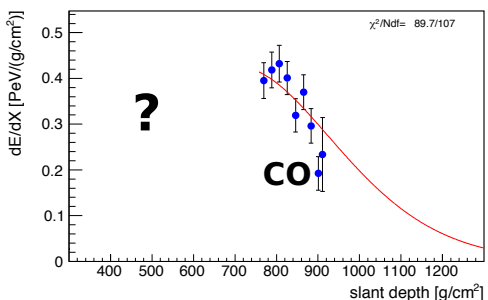
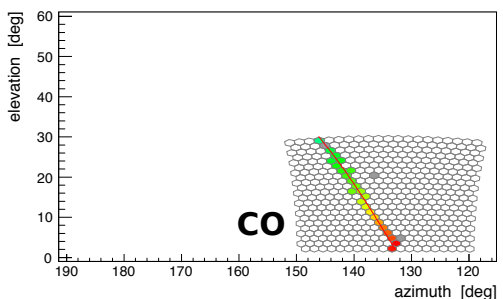
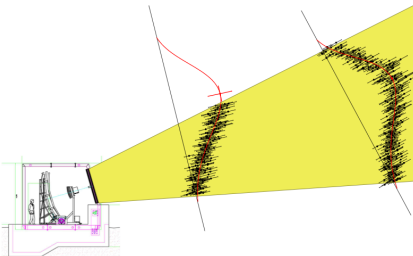
Backups

A. Porcelli for Pierre Auger | X_{max} above 10^{17} eV with the FD of the Pierre Auger Observatory (CR-EX 1176 – PoS 420)

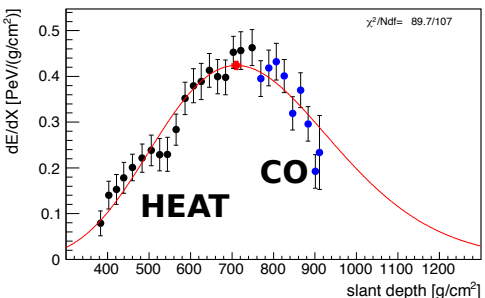
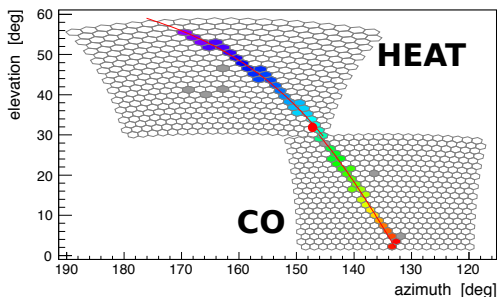
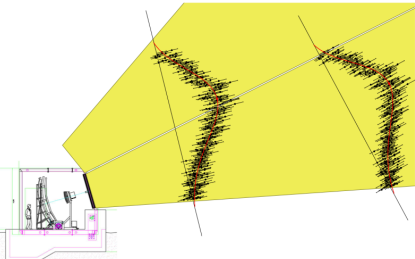
31.07.2015

2/11

HeCo (HEAT+CO): extended field of view



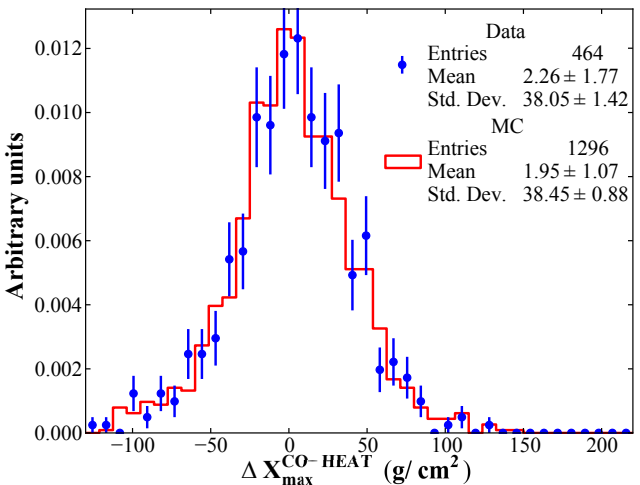
HeCo (HEAT+CO): extended field of view



HEAT in downward mode

Cross-checks with Coihueco (CO):

CO-HEAT (downward)



- ▶ X_{\max} difference between CO and HEAT compatible with reconstruction systematic uncertainties (see systematic uncertainties)
- ▶ Data and MC simulation are in agreement: good detector knowledge

Analysis Method

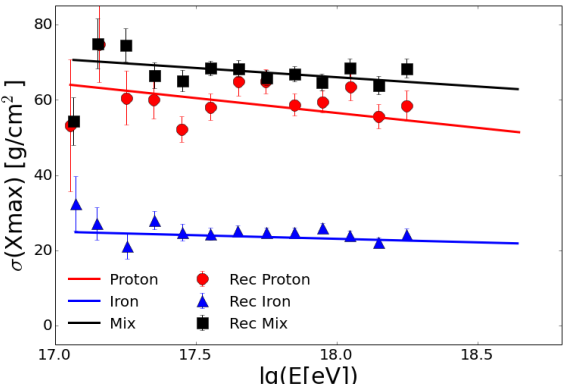
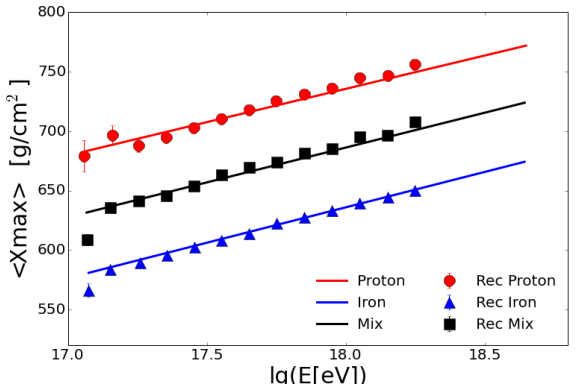
Same analysis method reported in Phys.Rev. D90 12 (2014) 122005 [[1409.4809v3](#)]

Overview of the data selection:

Good data taking condition	good data taking periods and good camera calibration constants require measured aerosol profile reject dust periods ($\text{VAOD}@3\text{km} < 0.1$) reject events with too much cloud contamination
Good X_{max} and Energy measurement	required hybrid geometry reconstruction Minimum track length observed X_{max} , with expected resolution $< 40 \text{ g cm}^{-2}$ reduced χ^2 of profile fit normal distributed
Field of view analysis	fiducial field of view to unbias the dataset
HeCo specific	considered higher trigger rate in Surface Detector stations for Fe-like events Surface Detector, HEAT and CO must be able to trigger simultaneously

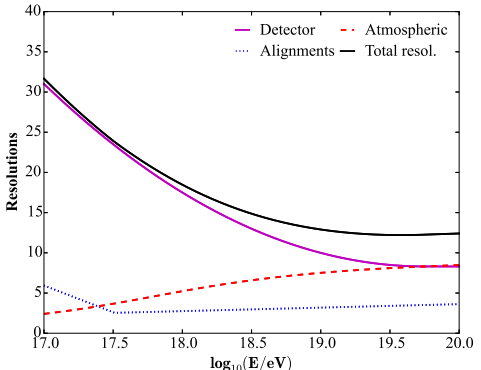
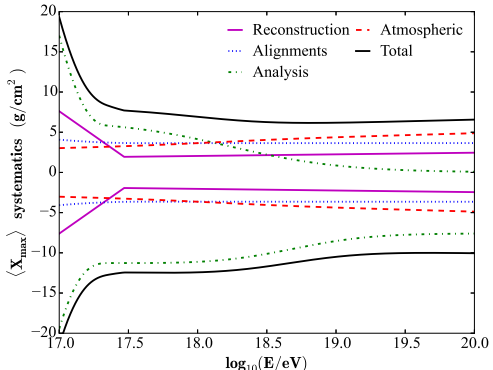
End-to-End cross-check with MC simulations

Proton, Iron and 50:50 mixture, generated (lines) VS reconstructed (markers)



Generated and reconstructed are compatible, with a residual bias in the lowest energy bin:
 correction using half of the 50:50 mixture (the largest),
 plus a symmetric systematic uncertainties accounted

$\langle X_{\max} \rangle$ systematic uncertainties & resolutions

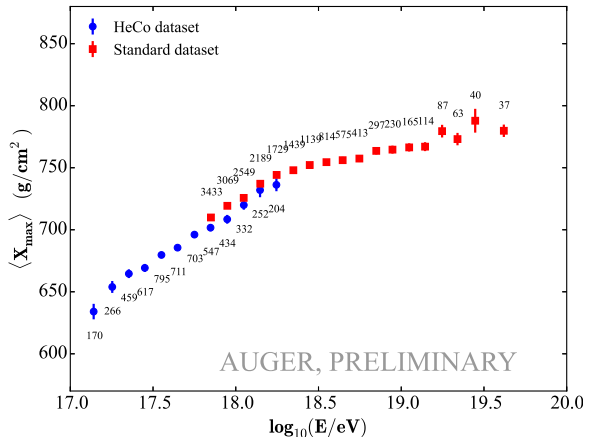


- ▶ reconstruction bias (only left) and detector resolution (right)
- ▶ offset in time between SD-FD, calibration and telescopes alignment
- ▶ analysis
- ▶ atmospheric uncertainty in the geometry reconstruction and fluorescence light yield

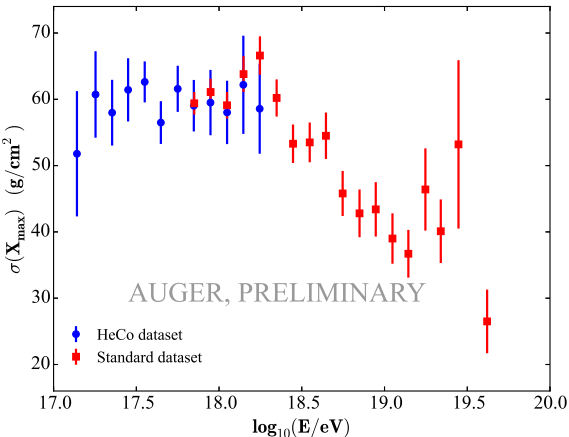
2 data set results...

Standard VS HeCo dataset

Average of X_{\max}

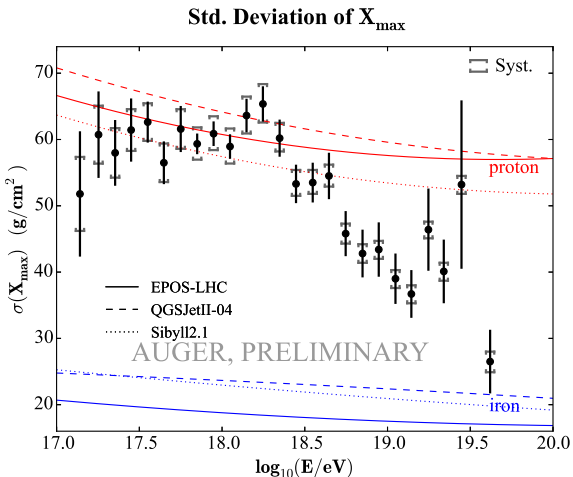
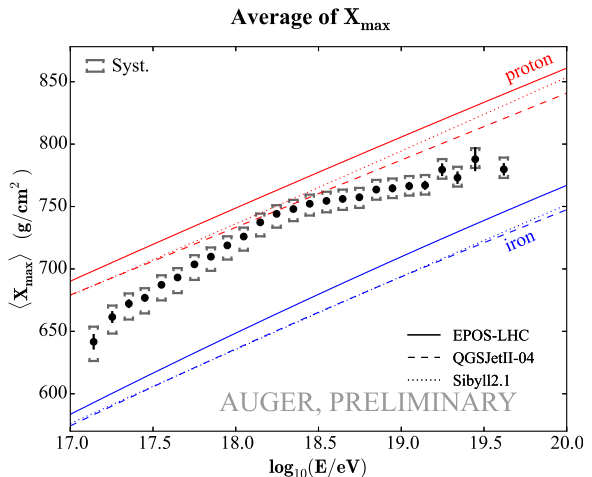


Std. deviation of X_{\max}



Compatibility inside the expected uncorrelated systematic uncertainties ($\sim 7 \text{ g cm}^{-2}$)

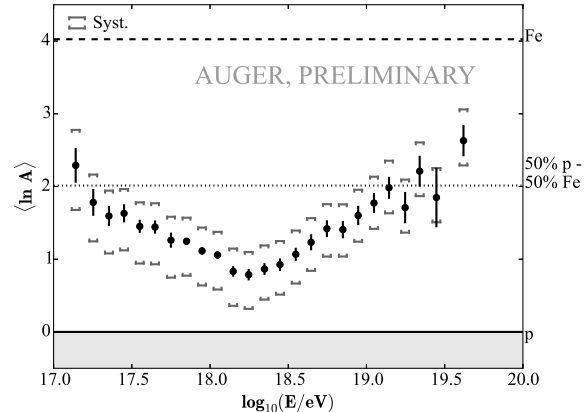
...merged together



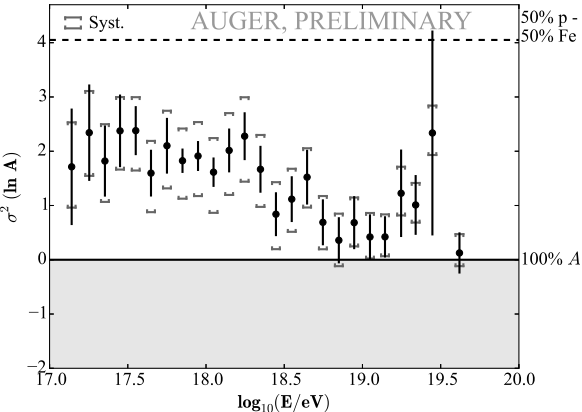
(with Proton and Iron pure composition for EPOS-LHC, Sibyll2.1, QGSJetII-04)

In A moments: EPOS-LHC

EPOS-LHC (Mean of ln A)



EPOS-LHC (Variance of ln A)



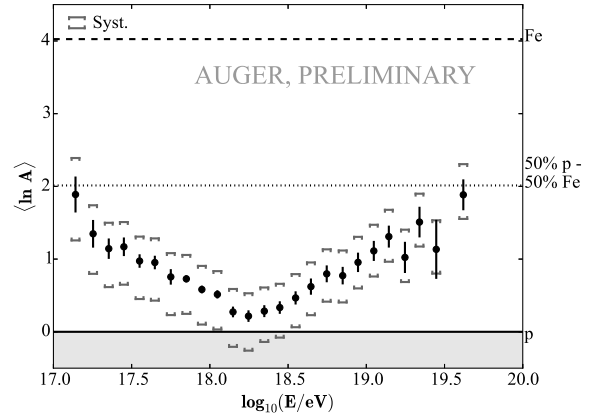
Low energy: largest mass dispersion, dominated by intermediate and heavy primaries

High energy: from the lightest at $\sim 10^{18.4}$ eV to heavier with less dispersion of masses.

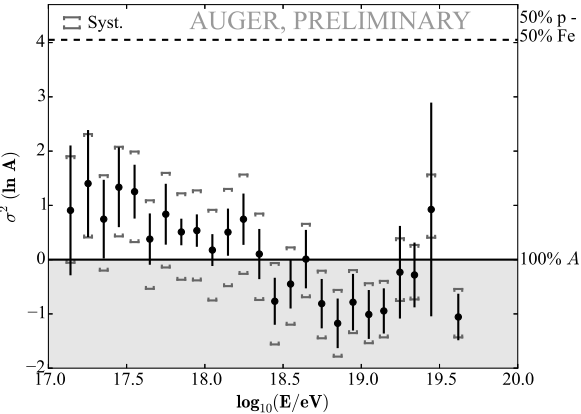
In A moments: QGSJetII-04



QGSJetII-04 (Mean of ln A)



QGSJetII-04 (Variance of ln A)

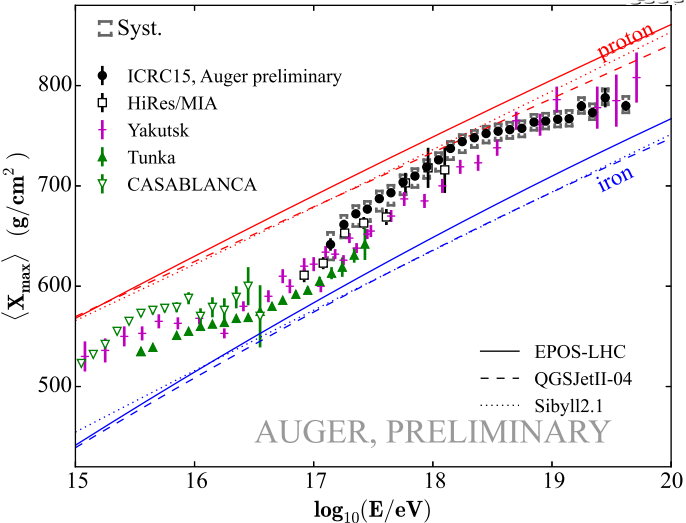


Low energy: largest mass dispersion, dominated by intermediate and heavy primaries

High energy: from the lightest at $\sim 10^{18.4}$ eV to heavier with less dispersion of masses.

Conclusions

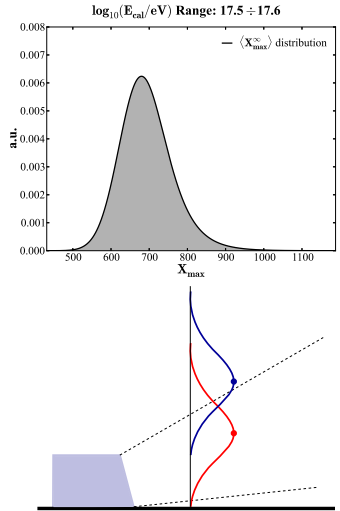
- ▶ X_{\max} measured in ~ 3 decades of energy (preliminary!): extend the lower energy range down to 10^{17} eV
- ▶ $\langle \ln A \rangle$ as a function of $\log(E/\text{eV})$ shows a non-constant composition in this energy range: the lightest at $\sim 10^{18.4}$ eV, heavier at lower and at higher energies



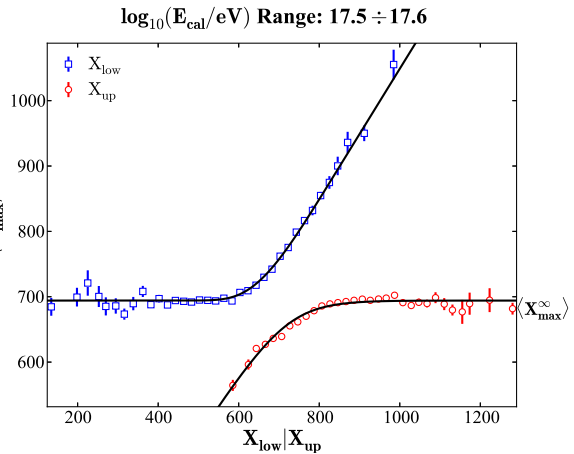
Backups

Study of the field of view bias

X_{\max} distribution



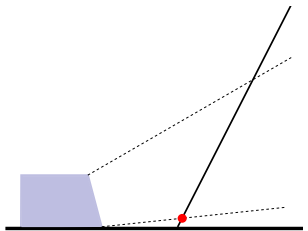
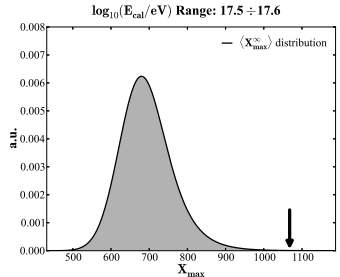
$\langle X_{\max} \rangle$ vs. X_{low} or X_{up} limit



No limit of the sample: asymptotic average $\langle X_{\max}^{\infty} \rangle$

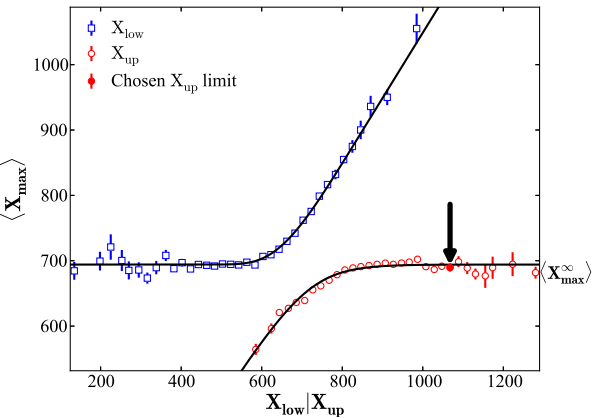
Study of the field of view bias

X_{\max} distribution



$\langle X_{\max} \rangle$ vs. X_{low} or X_{up} limit

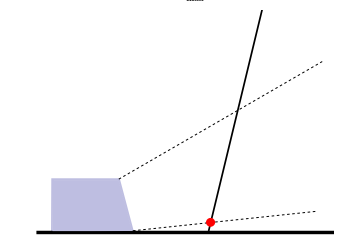
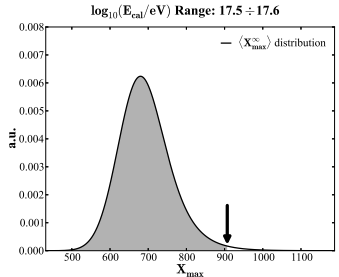
$\log_{10}(E_{\text{cal}}/\text{eV})$ Range: 17.5 ÷ 17.6



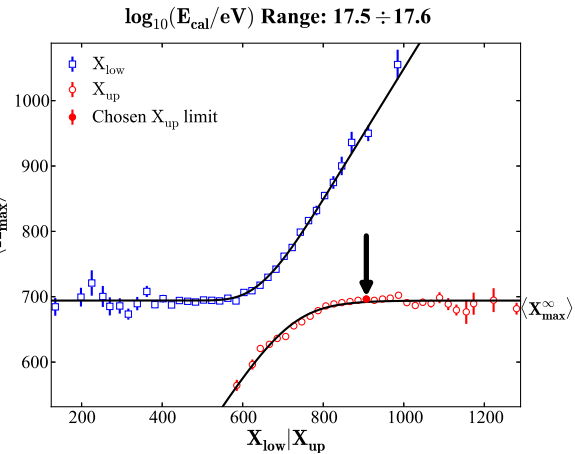
Large X_{up} : $\langle X_{\max} \rangle$ still $\langle X_{\max}^{\infty} \rangle$

Study of the field of view bias

X_{\max} distribution



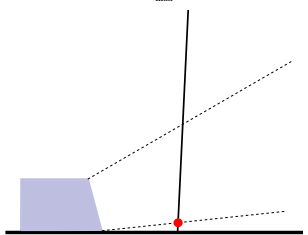
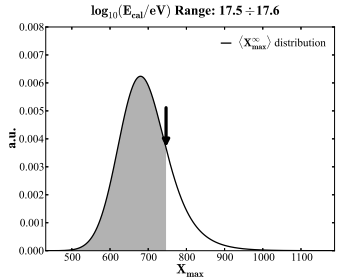
$\langle X_{\max} \rangle$ vs. X_{low} or X_{up} limit



Still $\langle X_{\max} \rangle \sim \langle X_{\max}^{\infty} \rangle$: need a study on the distribution tails?

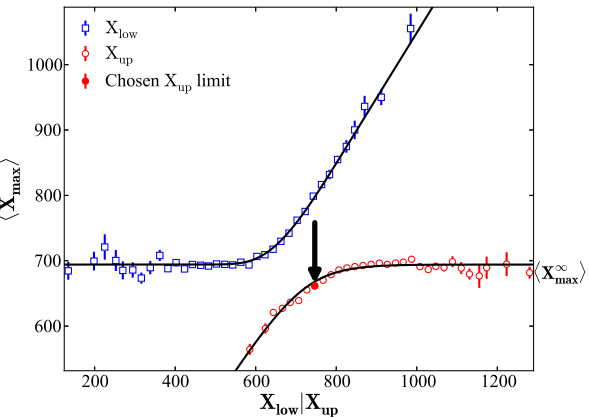
Study of the field of view bias

X_{\max} distribution



$\langle X_{\max} \rangle$ vs. X_{low} or X_{up} limit

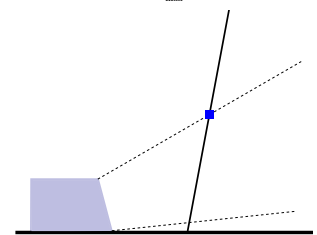
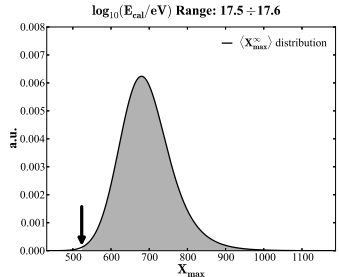
$\log_{10}(E_{\text{cal}}/\text{eV})$ Range: 17.5 ÷ 17.6



Too small X_{up} : $\langle X_{\max} \rangle < \langle X_{\max}^{\infty} \rangle$ (biased!)

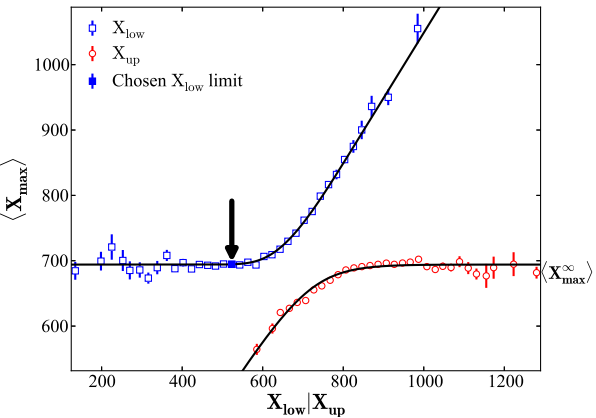
Study of the field of view bias

X_{\max} distribution



$\langle X_{\max} \rangle$ vs. X_{low} or X_{up} limit

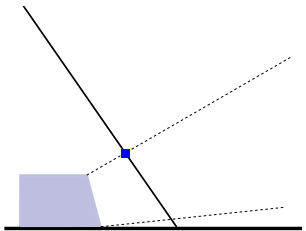
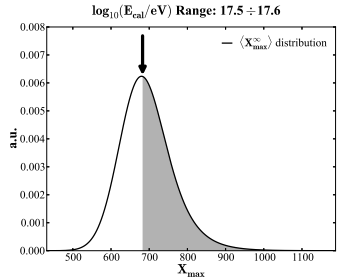
$\log_{10}(E_{\text{cal}}/\text{eV})$ Range: 17.5 ÷ 17.6



Small X_{low} : $\langle X_{\max} \rangle$ still $\langle X_{\max}^{\infty} \rangle$

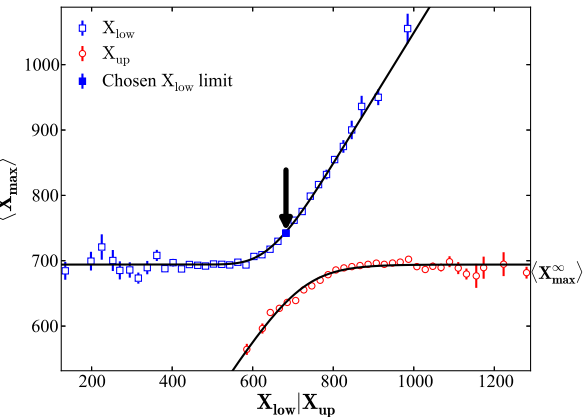
Study of the field of view bias

X_{\max} distribution



$\langle X_{\max} \rangle$ vs. X_{low} or X_{up} limit

$\log_{10}(E_{\text{cal}}/\text{eV})$ Range: 17.5 ÷ 17.6

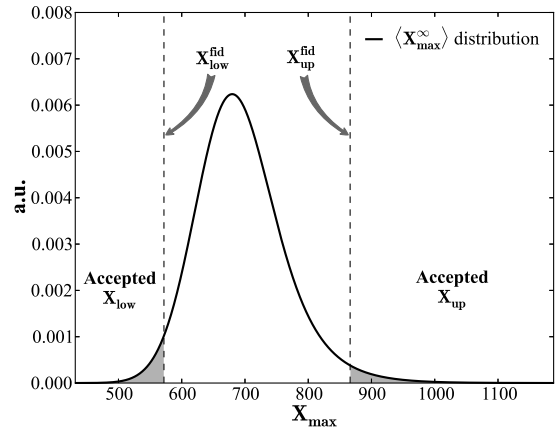


Too large X_{low} : $\langle X_{\max} \rangle > \langle X_{\max}^{\infty} \rangle$ (biased!)

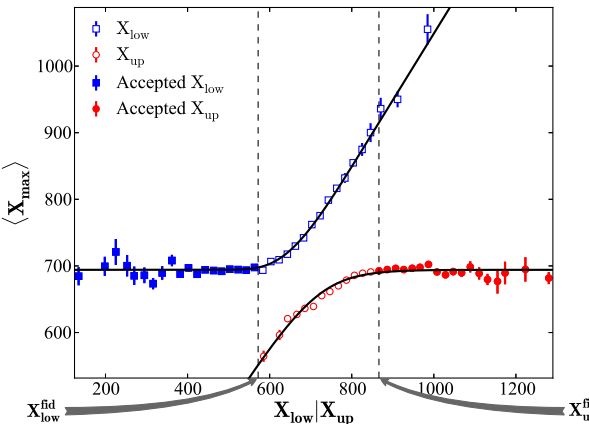
Fiducial field of view

The method uses the data itself optimizing the statistic

$\log_{10}(E_{\text{cal}}/\text{eV})$ Range: 17.5 ÷ 17.6



$\log_{10}(E_{\text{cal}}/\text{eV})$ Range: 17.5 ÷ 17.6



$X_{\text{low}} < X_{\text{low}}^{\text{fid}}$ and $X_{\text{up}} > X_{\text{up}}^{\text{fid}}$. $\langle X_{\max} \rangle \simeq \langle X_{\max}^{\infty} \rangle$ (unbiased!)